Coincidence measurements of the $(\pi^+,\pi^0 p)$ reaction at $T_{\pi^+}=165$ MeV

S. Høibråten,* S. Gilad, W. J. Burger,† and R. P. Redwine
Department of Physics and Laboratory for Nuclear Science, Massachusetts Institute of Technology, Cambridge, Massachusetts 02139

E. Piasetzky,‡ H. W. Baer, J. D. Bowman, F. H. Cverna, F. Irom,§ and M. J. Leitch
Los Alamos National Laboratory, Los Alamos, New Mexico 87545

J. N. Knudson**
Department of Physics, Arizona State University, Tempe, Arizona 85287

S. A. Wood††
School of Physics and Astronomy, Raymond and Beverly Sackler Faculty, Tel Aviv University, Ramat Aviv 69978, Israel

S. H. Rokni‡‡
Department of Physics, Utah State University, Logan, Utah 84322
(Received 24 September 1990)

We report coincidence measurements of the $(\pi^+,\pi^0 p)$ reaction at a beam energy of $T_{\pi^+}=165$ MeV. The neutral pions were detected by the LAMPF π^0 spectrometer and the protons by an array of plastic-scintillator telescopes. The resulting energy resolution for the determination of the excitation energy of the residual nucleus was about 10 MeV. Measurements were performed on ^{16}O at laboratory angles $\theta_{\pi^0}=70°$, 80°, 110°, and 130°. The cross section is predominantly quasifree. Its angular dependence follows the trend of the free single-charge-exchange cross section at back angles and is somewhat suppressed relative to this at more forward angles. Events corresponding to removal of p-shell nucleons were identified by their π^0 and p energies. The π^0 energy spectra for such events are compared to similar pion energy spectra for the ^{16}O$(\pi^\pm,\pi^\pm p)$ reactions; the cross-section ratios are consistent with ratios calculated from isospin coupling alone. π^0 energy spectra are also compared to predictions of Δ-hole model calculations; the calculations for events in which protons are detected at the conjugate quasifree angle underestimate the $(\pi^+,\pi^0 p)$ cross sections by 30–55 %. At $\theta_{\pi^0}=110°$ the $(\pi^+,\pi^0 p)$ reaction was also studied on Fe, Sn, and Pb. No significant A dependence of the cross section was observed.

I. INTRODUCTION

Various $(\pi,\pi' p)$ reactions have been studied for about 30 years (see, for example, Refs. 1 and 2). However, it is only over the last decade that kinematically complete coincidence measurements have been performed.[3–6] In particular, quasifree coincidence measurements give valuable information about nucleons inside the nucleus and their interactions with the remaining part of the nucleus. Such experiments have made a significant contribution to our understanding of medium-energy nuclear interactions.

In the energy range identified with the $\Delta(1232)$ resonance, such pion-induced nucleon removal processes are predominantly quasifree.[6,7] Ratios between inclusive cross sections $d\sigma/d\Omega_\pi$ for the $(\pi^+,\pi^+ p)$ and $(\pi^-,\pi^- p)$ reactions in the Δ-resonance region agree roughly with the corresponding ratios between the free $\pi^+ p$ and $\pi^- p$ cross sections,[7] while some very large deviations from these ratios have been found for exclusive cross sections $d^3\sigma/dE_\pi d\Omega_\pi d\Omega_p$.[3] These latter experimental ratios depend on the angle and energy of the ejected pion. The deviations are particularly interesting because some of the observed ratios of π^+-induced to π^--induced cross sections are several times larger than the corresponding ratio of free cross sections. Explanations based on initial-state interactions (pion charge exchange) or final-state interactions (nucleon charge exchange) are insufficient because such interactions in general can only decrease these cross section ratios. [The free $\pi^+ p$ cross section is essentially geometrical, and so modifications of this cross section can only contribute to a decrease of the ratios. The $(\pi^-,\pi^- p)$ cross section is increased by including the possibility of pion or nucleon charge exchange. This, of course, will also reduce the above cross-section ratios.] It is therefore clear that the elementary πp process must be substantially modified by the nuclear medium.[3,8]

Similar modifications would be expected for other πp isospin channels (cf. Ref. 8, which discusses this within the framework of the Δ-hole model), and we present here a study of the $(\pi^+,\pi^0 p)$ reaction at $T_{\pi^+}=165$ MeV. Earlier results obtained by our collaboration for ^{16}O$(\pi^+,\pi^0 p)$ at $T_{\pi^+}=245$ MeV indicated that the cross-section ratio of $(\pi^+,\pi^+ p)$ to $(\pi^+,\pi^0 p)$ for ^{16}O was significantly

different from the corresponding ratio of free cross sections at forward pion angles.[5] Some of the results presented in this paper were given earlier in a Brief Report;[6] most of the results are discussed in greater detail in Ref. 9.

II. EXPERIMENTAL APPARATUS

The experiment was performed at the low-energy pion (LEP) channel at the Clinton P. Anderson Meson Physics Facility (LAMPF). The layout of the experimental area is shown in Fig. 1. The two photons from the decay of the π^0 were detected with the LAMPF π^0 spectrometer,[10] and the protons were detected with an array of plastic-scintillator telescopes. The measurements were done at π^0 laboratory angles of 70°, 80°, 110°, and 130°.

The beam flux was typically 10^7 π^+/s. It was monitored by a toroid loop around the primary proton beam. This monitor was frequently calibrated to the pion flux by measuring the ^{11}C activity from the reaction ^{12}C($\pi^{\pm}$,X)^{11}C and comparing it to known cross sections.[11]

The π^0 spectrometer operated in its vertical opening angle configuration. At each π^0 angle, the spectrometer was set to optimize the acceptance for the range of π^0 energies expected from the quasifree process. The spectrometer solid angle was maximized while maintaining π^0 energy resolution at about 8 MeV. The energy calibration of the π^0 spectrometer was checked using π^0's from the reaction $\pi^- p \rightarrow \pi^0 n$. The measured π^0 energies agreed within 2 MeV with values expected from two-body kinematics. All results presented below are based on π^0's collected from a region of $\pm 12°$ around the central π^0 angle.

The energy-dependent acceptance of the π^0 spectrometer was calculated using the Monte Carlo simulation code PIANG.[10,12] Results for all our setups are shown in Fig. 2. Clearly, the acceptance was significantly reduced outside a band of approximately 100 MeV width. However, this energy range, in which reliable data could be obtained, was still wide enough to comfortably include essentially the whole quasifree peak in all our measurements.

The product of solid angle and spectrometer efficiency

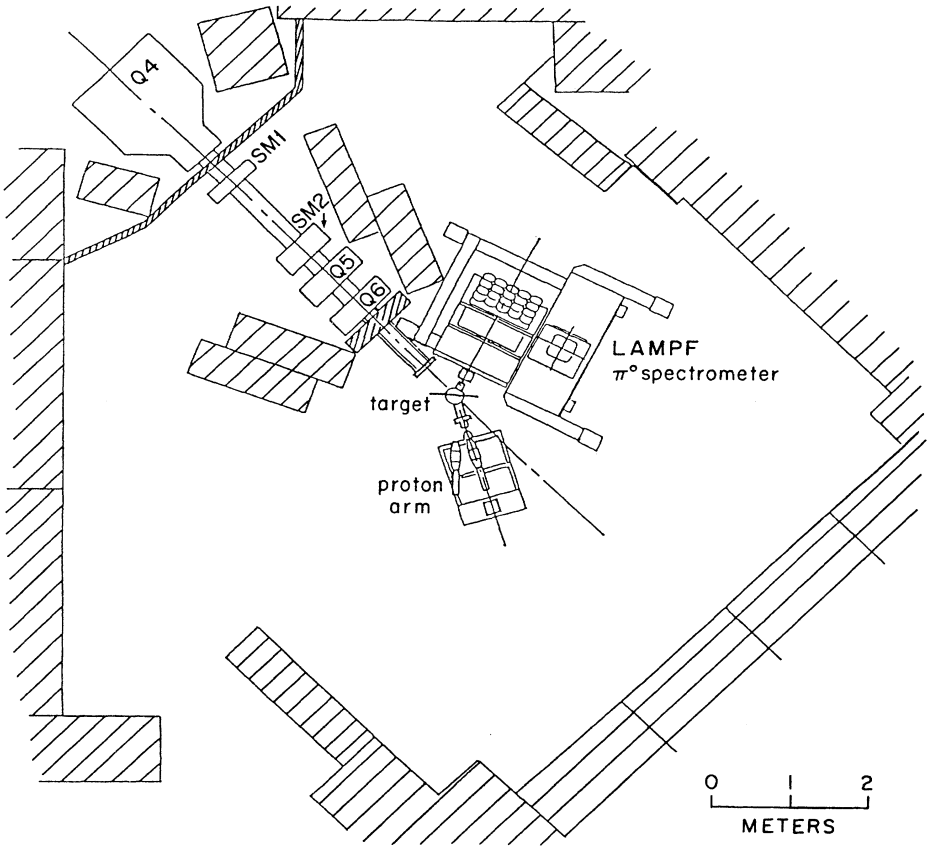

FIG. 1. Floor layout of the experimental area. The figure shows the extension of the LEP beam channel with its magnets, the target, the particle detectors, and the main shielding. $Q4$ is the last quadrupole magnet in the standard beam channel; $Q5$ and $Q6$ were installed to improve focusing at the target. SM1 and SM2 are steering magnets. The shielding is indicated by the hatched areas. The more densely hatched areas indicate Pb shielding; the remaining shielding was provided by concrete blocks. The most downstream part of the beam pipe (after $Q6$) was made of Pb.

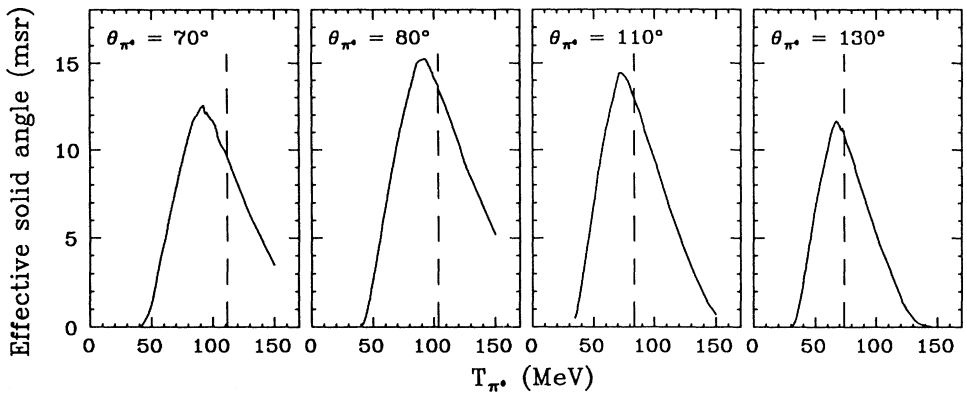

FIG. 2. Calculated π^0 spectrometer energy acceptance for all setups. The curves show the effective solid angle covered by the spectrometer as a function of the kinetic energy of the ejected π^0's. The results shown are for the water targets. (The changes caused by using other targets are minor.) All calculations assumed a π^0 spectrometer angular acceptance of $\pm 12°$ around the nominal π^0 angle, as well as a maximum (cutoff) value of 0.25 for the decay-photon energy-sharing parameter $(E_{\gamma_1}-E_{\gamma_2})/(E_{\gamma_1}+E_{\gamma_2})$. The calculated acceptances are larger at $\theta_{\pi^0}=80°$ and 110° mainly because the distance from the target to the spectrometer was shorter here than in the other setups. The dashed lines indicate the quasifree energy.

was also determined experimentally, using the reaction $\pi^- p \rightarrow \pi^0 n$ on a CH_2 target (and on a ^{12}C target for background subtraction). When the energy dependence of the spectrometer solid angle had been accounted for (cf. Fig. 2), the remaining π^0 spectrometer efficiency was found to be approximately constant and in agreement with previous measurements.[13]

The protons were detected by a vertical array of seven telescopes covering an angular range of $\pm 51°$ around the nominal free proton emission angle (later referred to as the quasifree angle θ_{qf}). An eighth proton telescope was positioned in the scattering (horizontal) plane 17° back from this angle. The vertical configuration of the array allowed measurements over the complete quasifree angular correlation region for a wide range of π^0 angles while still keeping the π^+ beam from hitting the proton detectors directly. Each telescope consisted of a ΔE and an E plastic scintillator with thicknesses 0.3 and 20.3 cm, respectively. This allowed excellent particle detection and identification over all proton energies above approximately 30 MeV. Each proton telescope covered a solid angle of 8.5 msr. The solid angles of the E detectors were larger than those of the ΔE's in order to avoid protons leaking out the sides. The full width at half maximum (FWHM) energy resolution of the proton detectors was about 3 MeV. The proton detectors were calibrated using monoenergetic protons. These protons were taken either directly from the LEP beam channel or from the reaction $\pi^+ d \rightarrow 2p$, using a CD_2 target and detecting two-proton coincidence events. We estimate about 1 MeV uncertainty in the proton energy calibration.

Four target materials were used for the coincidence measurements: water, natural Fe (0.902 g/cm^2), natural Sn (2.05 g/cm^2), and natural Pb (1.160 g/cm^2). The water targets were water-filled rectangular boxes with 50-μm Mylar windows. For these targets, the target thickness and target angle were chosen for each measurement to maximize the counting rate while maintaining energy resolution for the determination of the excitation energy of the residual nucleus at about 10 MeV. The thicknesses

TABLE I. Physical setup parameters. The parameters listed are the central π^0 angle θ_{π^0}, the π^0 spectrometer opening angle η_{π^0} and the corresponding optimal π^0 kinetic energy T_{π^0}, the distance from the target to the π^0 spectrometer r_{π^0}, the proton angle θ_p for the central proton detector, the target angle θ_t (the angle between the beam and a normal to the target on the downstream side), and the thickness $(\rho t)_t$ of the water target used. Positive angles indicate beam right, and negative angles indicate beam left. The proton arm and π^0 spectrometer swapped sides for the measurement at $\theta_{\pi^0}=70°$ to make better use of the space available.

θ_{π^0} (deg)	η_{π^0}/T_{π^0} (deg)/(MeV)	r_{π^0} (cm)	θ_p (deg)	θ_t (deg)	$(\rho t)_t$ (g/cm^2)
70.0	73.73/90.0	60.0	−47.6	−52.0	0.32±0.03
−80.0	73.73/90.0	50.0	42.3	50.0	0.58±0.03
−110.0	81.40/72.0	50.0	27.9	55.0	0.59±0.03
−129.7	84.90/65.0	60.0	19.45	35.0	0.90±0.05

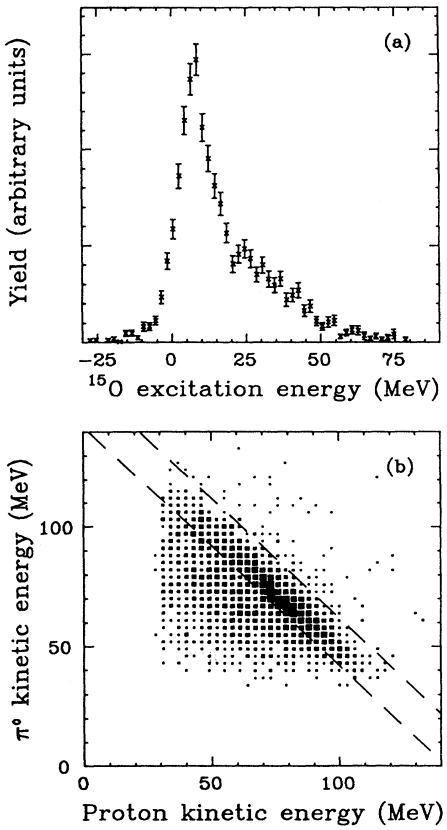

FIG. 3. Data from the $^{16}O(\pi^+,\pi^0 p)^{15}O$ reaction obtained at $\theta_{\pi^0}=110°$ with the proton detected at the conjugate quasifree angle. (a) Excitation energy of the residual ^{15}O nucleus. (b) Correlation of π^0 kinetic energy versus proton kinetic energy. The range between the dashed lines represents our estimate of events due to p-shell nucleon removal.

of the water targets varied from about 3 to about 10 mm and were in each case established to better than 10% accuracy by comparing measurements of the $\pi^- p \rightarrow \pi^0 n$ reaction on the hydrogen in the water to known cross sections.[14] These measurements also gave direct values for the product of target thickness and spectrometer efficiency for use in the analysis of the coincidence data. The hydrogen content of the water targets was, of course, of no concern for our study of the $(\pi^+,\pi^0 p)$ reaction.

The values of the physical setup parameters for all our measurements are listed in Table I. This table also lists the measured thicknesses of the water targets used in the experiment.

III. DATA ANALYSIS

A typical spectrum of the excitation energy of the residual ^{15}O nucleus from the reaction $^{16}O(\pi^+,\pi^0 p)$ is presented in Fig. 3(a). The most pronounced peak corresponds to the removal of nucleons from the p shell (the $p_{1/2}$ and $p_{3/2}$ levels were not resolved). In the analysis we attempted to separate such p-shell events from events due to other processes by applying a cut in a histogram of the detected π^0 energy versus the energy of the coincident proton. This is shown in Fig. 3(b) for the same events as in Fig. 3(a). From varying the position of the p-shell cut for a number of cases, we estimate about 12% uncertainty in the extracted cross sections due to reasonable variations of this cut. Furthermore, from fitting a sum of Gaussian distributions to the shape of the excitation energy spectrum of Fig. 3(a), we estimate that typically 20% of the events included in the cross sections for p-shell nucleon removal are most likely due to other processes.

The cross sections presented below for p-shell nucleon removal have been corrected for losses due to nuclear interaction in the E detectors.[15,16] This correction varies from less than 1% to more than 15% in our energy range, the exact value depending on the kinetic energy of the proton. The correction does not apply to cross sections summed over all detected protons, as inelastic nuclear interactions reduce the average measured energy of the detected protons, but do not appreciably affect the total number of events detected above our threshold.

All cross sections were first corrected for the energy-dependent π^0 spectrometer acceptance (by using the Monte Carlo code PIANG), and for accidental $\pi^0 p$ coincidences (typically about 1.5%). We then subtracted background events (obtained using an empty water target or no target at all). The background contribution varied from 4% at $\theta_{\pi^0}=130°$ to 15% at $\theta_{\pi^0}=70°$. The resulting spectra were corrected for losses due to attenuation of the π^0 decay photons in the targets[17] (the attenuation losses in the rest of the system were implicitly included in the experimentally determined π^0 spectrometer efficiency discussed above). The photon attenuation losses were small in the water targets (1–3 %), but they became significant for the heavier targets (about 13% for Pb).

IV. RESULTS

A. Cross sections $d^3\sigma/dE_{\pi^0} d\Omega_{\pi^0} d\Omega_p$

In this experiment we made direct measurements of the quadruply differential cross sections $d^4\sigma/dE_{\pi^0} dE_p d\Omega_{\pi^0} d\Omega_p$ [cf. Fig. 3(b)]. The $d^3\sigma/dE_{\pi^0} d\Omega_{\pi^0} d\Omega_p$ spectra discussed below were obtained by summing over all detected proton energies (after having made those cuts and corrections described above that depend explicitly on the energy of the proton).

1. Dependence on scattering angle

$^{16}O(\pi^+,\pi^0 p)$ measurements using water targets were made at all π^0 angles studied in the experiment. Figure 4 shows $d^3\sigma/dE_{\pi^0} d\Omega_{\pi^0} d\Omega_p$ spectra for the $^{16}O(\pi^+,\pi^0 p)$ reaction as a function of T_{π^0} for the central proton telescope (at the quasifree angle) in all setups. The data have been cut on p-shell nucleon removal. Because of the p-shell momentum distribution, one expects to see a dip in the cross section near the quasifree energy for small solid angle detectors. Our data do not display much of this p-

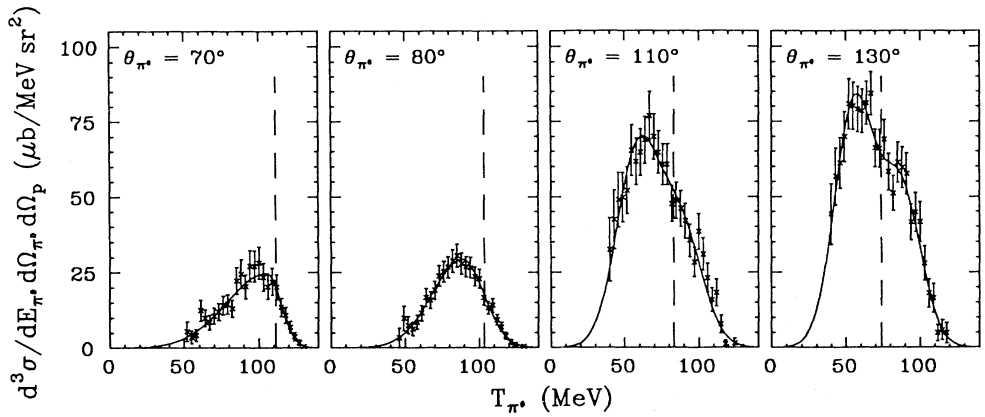

FIG. 4. Energy spectra for the $^{16}O(\pi^+,\pi^0 p)$ reaction. Only p-shell nucleon removal events collected using the proton telescope at the conjugate quasifree angle are included. The dashed lines indicate the quasifree energy. The solids lines are fits to the data. The fits for the two forward π^0 angles are asymmetric Gaussians, while a sum of two symmetric Gaussians was used for the backward angles. There is a 15% normalization uncertainty in addition to the uncertainties shown in the figure.

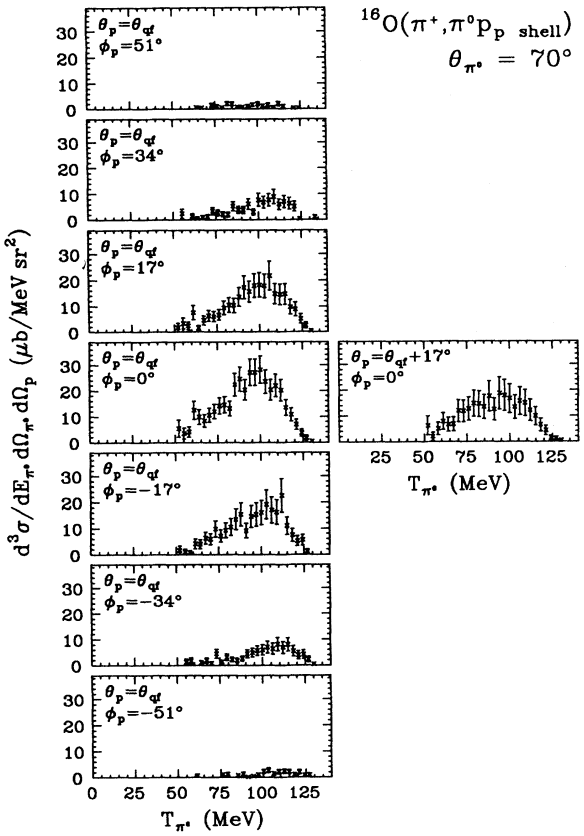

FIG. 5. p-shell nucleon removal spectra at $\theta_{\pi^0}=70°$. The position of each proton telescope is indicated by the angles θ_p (measured in the scattering plane) and ϕ_p (measured perpendicular to the scattering plane). The normalization uncertainty (15%) is not included in the figure.

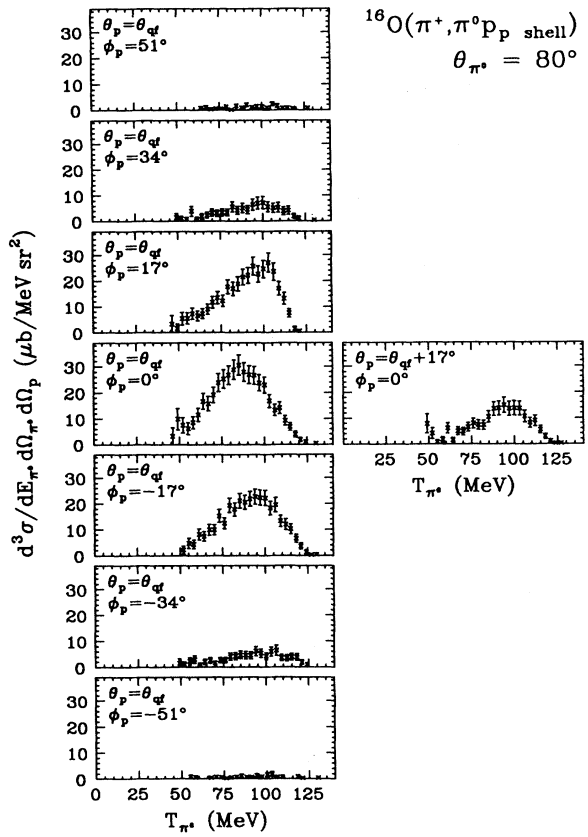

FIG. 6. p-shell nucleon removal spectra at $\theta_{\pi^0}=80°$. The position of each proton telescope is indicated by the angles θ_p (measured in the scattering plane) and ϕ_p (measured perpendicular to the scattering plane). The normalization uncertainty (15%) is not included in the figure.

shell signature. This is presumably due to the nonzero solid angles of the detectors, as well as to the above mentioned 20% contribution from processes other than p-shell nucleon removal. In particular, s-shell nucleon removal events will peak around the quasifree energy.

The spectra in Fig. 4 are all plotted on the same scale. We note that the cross section is significantly larger at the backward π^0 angles than at the more forward angles. This is similar to the behavior of the free πN cross sections.[14]

$d^3\sigma/dE_{\pi^0}d\Omega_{\pi^0}d\Omega_p$ spectra for p-shell nucleon removal for all telescopes are shown in Figs. 5–8. The arrangement of the spectra in each figure reflects the arrangement of the corresponding telescopes in the proton arm. The lower three of these spectra were obtained by the telescopes below the scattering plane; next follow the telescopes in the scattering plane (the telescopes at the quasifree angle and one positioned at a larger scattering angle than the main array); and then the telescopes above the scattering plane. Note our definition of the proton angles θ_p and ϕ_p: θ_p is measured in the scattering plane ("longitude") and ϕ_p is measured perpendicularly to this ("latitude"). We see that the $\pi^0 p$ angular correlation has its maximum at the quasifree angle (the central telescope) for all our measurements, thus confirming the quasifree nature of the $(\pi^+,\pi^0 p)$ reaction at this energy. Furthermore, all results are quite symmetric about the scattering plane. The position of the p-shell peak appears to shift towards higher π^0 energies as the out-of-plane angle increases. This is to be expected since the proton angle with respect to the beam increases with the out-of-plane angle. Kinematically, increasing the out-of-plane angle would therefore favor lower-energy protons or equivalently, higher-energy pions. The statistics in the extreme out-of-plane spectra are too low to permit discussion of spectral features, but these spectra still provide important information about the absolute size of the cross sections at these angles.

Similar $d^3\sigma/dE_{\pi^0}d\Omega_{\pi^0}d\Omega_p$ spectra including all good $\pi^0 p$ events are shown in Figs. 9–12. Comparing with the

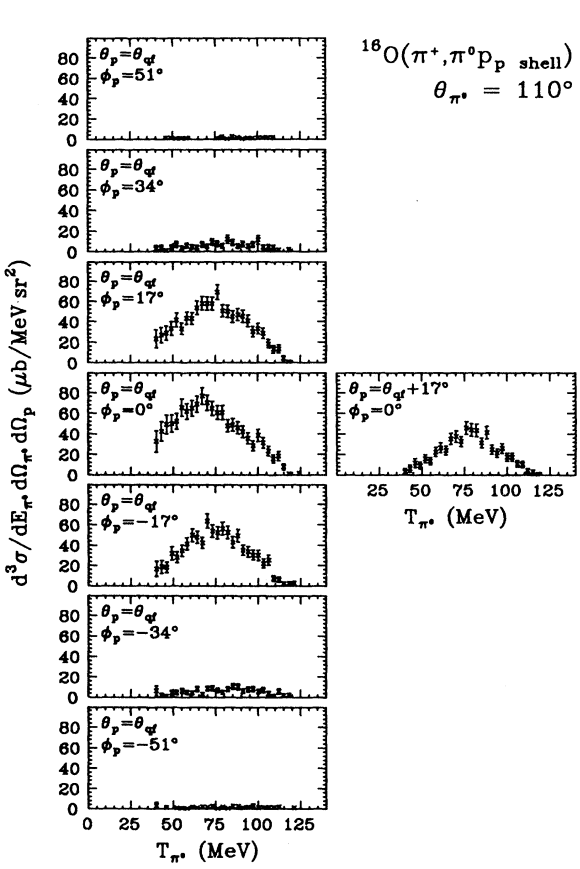

FIG. 7. p-shell nucleon removal spectra at $\theta_{\pi^0}=110°$. The position of each proton telescope is indicated by the angles θ_p (measured in the scattering plane) and ϕ_p (measured perpendicular to the scattering plane). The normalization uncertainty (15%) is not included in the figure.

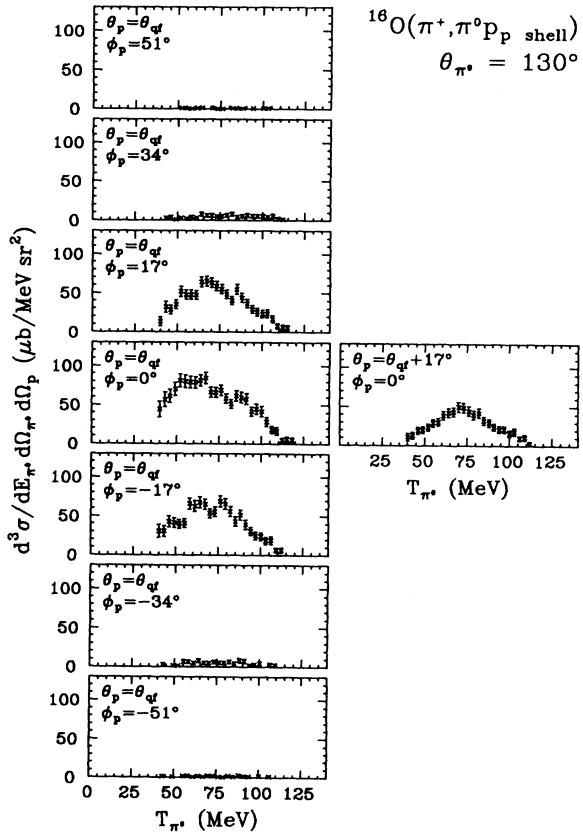

FIG. 8. p-shell nucleon removal spectra at $\theta_{\pi^0}=130°$. The position of each proton telescope is indicated by the angles θ_p (measured in the scattering plane) and ϕ_p (measured perpendiuclar to the scattering plane). The normalization uncertainty (15%) is not included in the figure.

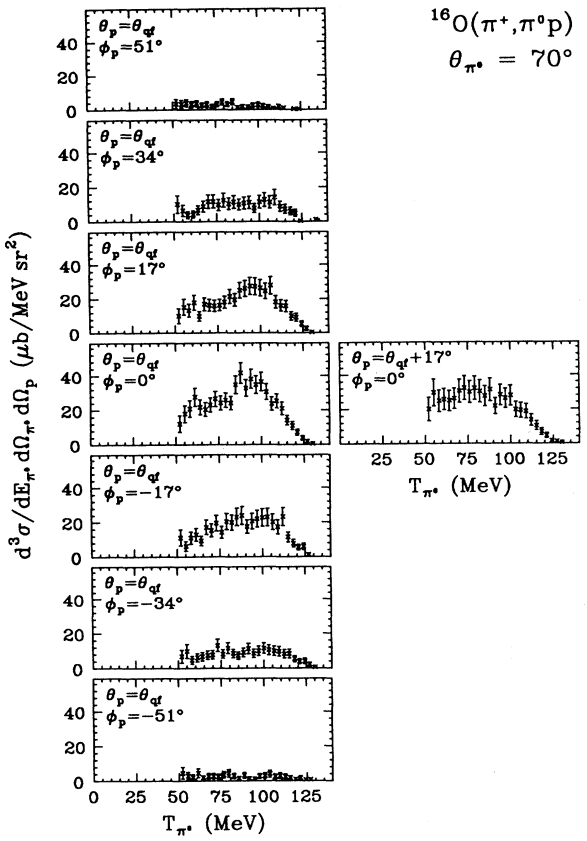

FIG. 9. Complete spectra at $\theta_{\pi^0}=70°$. The position of each proton telescope is indicated by the angles θ_p (measured in the scattering plane) and ϕ_p (measured perpendicular to the scattering plane). The normalization uncertainty (9%) is not included in the figure.

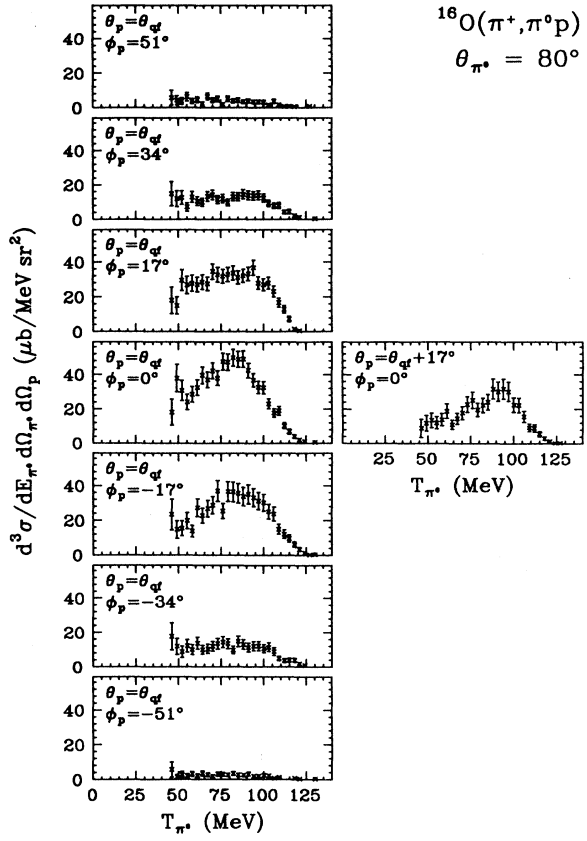

FIG. 10. Complete spectra at $\theta_{\pi^0}=80°$. The position of each proton telescope is indicated by the angles θ_p (measured in the scattering plane) and ϕ_p (measured perpendicular to the scattering plane). The normalization uncertainty (8%) is not included in the figure.

spectra for p-shell nucleon removal in Figs. 5–8, we note an increase in the cross section at lower values of T_{π^0}. This indicates the expected larger contribution from more deeply inelastic processes.

2. *A Dependence*

At $\theta_{\pi^0}=110°$, we collected data on the A dependence of the $(\pi^+,\pi^0 p)$ reaction. In addition to the measurements on ^{16}O presented above, we measured the reaction on three other targets: Fe, Sn, and Pb.

Our results for $d^3\sigma/dE_{\pi^0} d\Omega_{\pi^0} d\Omega_p$ for the proton detector at the conjugate quasifree angle for the four targets are shown in Fig. 13. Our data do not permit identification of nucleon removal from specific nuclear shells; all good $\pi^0 p$ events are therefore included in the spectra. The cross sections are remarkably similar in magnitude even though our measurements span a range of A from 16 to 208.

The complete set of cross-section spectra for all proton telescopes for the Fe, Sn, and Pb targets are presented in Figs. 14–16. The corresponding information for ^{16}O is found in Fig. 11.

B. Integrated cross sections $d^2\sigma/d\Omega_{\pi^0} d\Omega_p$ and $d\sigma/d\Omega_{\pi^0}$

To obtain better information about the $\pi^0 p$ angular correlation, we integrated the $d^3\sigma/dE_{\pi^0} d\Omega_{\pi^0} d\Omega_p$ cross sections over all π^0 kinetic energies. The tails of the energy spectra are missing because the energy acceptances of the π^0 spectrometer and the proton arm discriminate against certain energy ranges; it was therefore necessary to fit a mathematical function to the data in order to perform this integration. We found that either an asymmetric Gaussian or a sum of two symmetric Gaussians was best suited for the purpose. We ultimately used the sum of two Gaussians for all complete (no p-shell cut) spectra as well as for the p-shell nucleon removal spectra taken at $\theta_{\pi^0}=110°$ and 130°. Some of the fits are shown in Figs. 4 and 13.

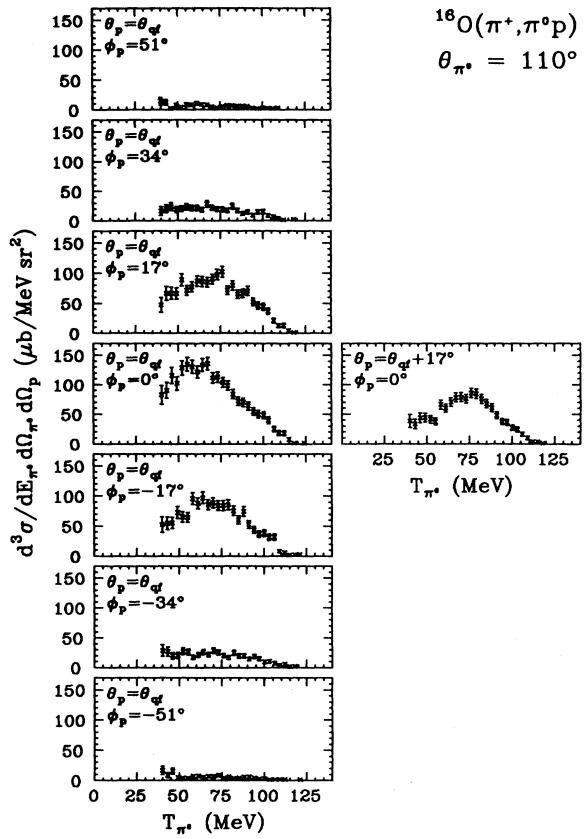

FIG. 11. Complete spectra at $\theta_{\pi^0}=110°$. The position of each proton telescope is indicated by the angles θ_p (measured in the scattering plane) and ϕ_p (measured perpendicular to the scattering plane). The normalization uncertainty (9%) is not included in the figure.

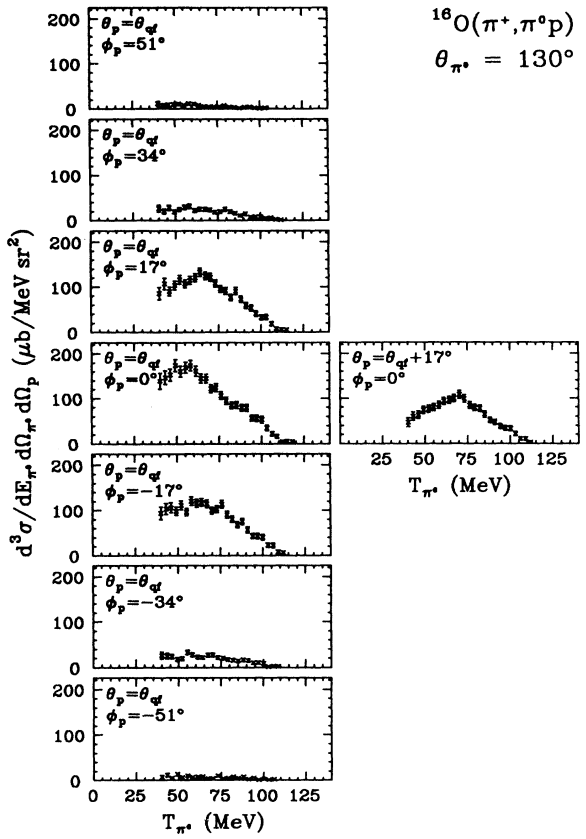

FIG. 12. Complete spectra at $\theta_{\pi^0}=130°$. The position of each proton telescope is indicated by the angles θ_p (measured in the scattering plane) and ϕ_p (measured perpendicular to the scattering plane). The normalization uncertainty (8%) is not included in the figure.

TABLE II. Integrated cross sections $d^2\sigma/d\Omega_{\pi^0}d\Omega_p$ and $d\sigma/d\Omega_{\pi^0}$ for p-shell nucleon removal events. The position of each proton telescope is indicated by the angles θ_p (measured in the scattering plane) and ϕ_p (measured perpendicular to the scattering plane). Only the measurements made at $\theta_p=\theta_{qf}$ were used in calculating $d\sigma/d\Omega_{\pi^0}$. There is a normalization uncertainty of 15% in addition to the uncertainties quoted in the table.

		$d^2\sigma/d\Omega_{\pi^0}d\Omega_p$ for $^{16}O(\pi^+,\pi^0p_{p\text{-shell}})$ (mb/sr^2)			
θ_p (deg)	ϕ_p (deg)	$\theta_{\pi^0}=70°$	$\theta_{\pi^0}=80°$	$\theta_{\pi^0}=110°$	$\theta_{\pi^0}=130°$
θ_{qf}	51	0.07±0.01	0.06±0.01	0.10±0.02	0.04±0.01
θ_{qf}	34	0.26±0.02	0.27±0.02	0.42±0.08	0.32±0.03
θ_{qf}	17	0.76±0.05	1.03±0.04	3.05±0.13	2.99±0.10
θ_{qf}	0	1.14±0.06	1.30±0.05	3.70±0.14	4.46±0.15
θ_{qf}	−17	0.71±0.05	1.00±0.04	2.70±0.10	3.19±0.10
θ_{qf}	−34	0.26±0.02	0.26±0.02	0.44±0.04	0.29±0.03
θ_{qf}	−51	0.08±0.01	0.05±0.01	0.10±0.02	0.09±0.02
θ_{qf}+17	0	0.80±0.06	0.53±0.03	1.71±0.07	2.09±0.14
$d\sigma/d\Omega_{\pi^0}$ (mb/sr)		0.71±0.05	0.94±0.05	2.15±0.08	2.14±0.05

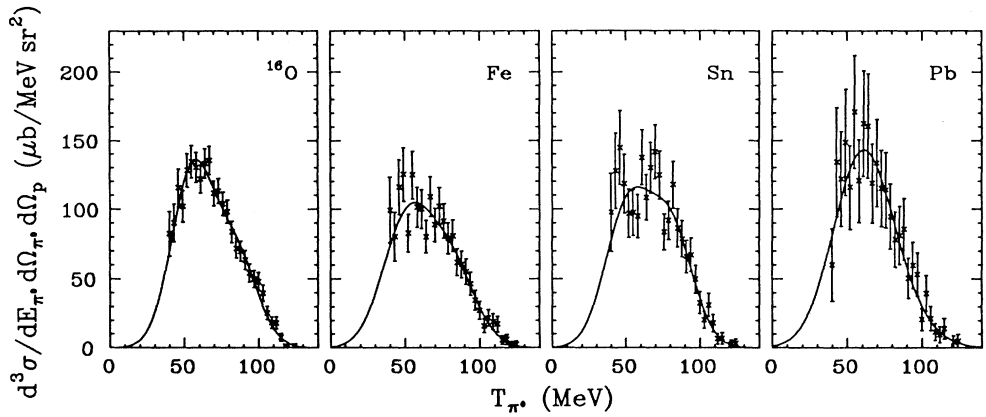

FIG. 13. Energy spectra for the $(\pi^+,\pi^0 p)$ reaction on various targets. All data are for $\theta_{\pi^0}=110°$, and they were collected using the proton telescope at the conjugate quasifree angle. The solid lines are fits to the data. A sum of two Gaussians was used for all fits. The normalization uncertainty (9% for oxygen and 10% for the other targets) is not included in the figure.

The cross sections $d^2\sigma/d\Omega_{\pi^0}d\Omega_p$ obtained by integrating the fitted functions over all T_{π^0} are listed in Tables II–IV. Those cross sections corresponding to the telescopes in the vertical array are plotted as a function of the proton out-of-plane angle in Figs. 17–19. The cross sections all peak at the quasifree angle, and they are clearly symmetric about the scattering plane.

To enable a more quantitative description of the angular correlation, we fit a Gaussian function on top of a constant background to our results for $d^2\sigma/d\Omega_{\pi^0}d\Omega_p$. A similar description has been used in earlier πp work.[7] We see from Figs. 18 and 19 that the angular distribution is described well by this function when no p-shell cut is imposed on the data. The width of the Gaussian is quite consistent with that expected from a Fermi momentum distribution. The p-shell nucleon removal results shown in Fig. 17, however, appear not to be Gaussian near the peak. This feature is in qualitative agreement with a p-shell nucleon momentum distribution; the probability of scattering near the quasifree angle is low. In all cases the background is small compared to the peaked part of the cross section.

We may now calculate the cross section $d\sigma/d\Omega_{\pi^0}$ for the quasifree part of the $(\pi^+,\pi^0 p)$ reaction by integrating the Gaussian part of the fitted curves in Figs. 17–19 over all proton directions. We assume, consistent with data from the $(\pi^+,\pi^+ p)$ reaction,[7] that the quasifree angular correlation is roughly the same in plane and out of plane in the laboratory frame. The results are listed at the bottom of Tables II–IV. We note that the fraction of p-shell removal events in the $^{16}O(\pi^+,\pi^0 p)$ reaction is roughly the same for all π^0 angles, about 40–50 %. This relative-

TABLE III. Integrated cross sections $d^2\sigma/d\Omega_{\pi^0}d\Omega_p$ and $d\sigma/d\Omega_{\pi^0}$ for all coincidence events. The position of each proton telescope is indicated by the angles θ_p (measuring in the scattering plane) and ϕ_p (measured perpendicular to the scattering plane). Only the measurements made at $\theta_p=\theta_{qf}$ were used in calculating $d\sigma/d\Omega_{\pi^0}$. There is a normalization uncertainty of 9% for the measurements at $\theta_{\pi^0}=70°$ and $\theta_{\pi^0}=110°$ and 8% for the other measurements in addition to the uncertainties quoted in the table.

		$d^2\sigma/d\Omega_{\pi^0}d\Omega_p$ for $^{16}O(\pi^+,\pi^0 p)$ (mb/sr^2)			
θ_p (deg)	ϕ_p (deg)	$\theta_{\pi^0}=70°$	$\theta_{\pi^0}=80°$	$\theta_{\pi^0}=110°$	$\theta_{\pi^0}=130°$
θ_{qf}	51	0.17±0.02	0.25±0.03	0.40±0.08	0.42±0.04
θ_{qf}	34	0.60±0.04	0.80±0.04	1.33±0.09	1.38±0.08
θ_{qf}	17	1.34±0.06	1.90±0.07	5.17±0.22	6.50±0.18
θ_{qf}	0	1.79±0.07	2.40±0.07	6.89±0.22	8.78±0.28
θ_{qf}	−17	1.17±0.07	1.83±0.08	4.82±0.22	6.39±0.19
θ_{qf}	−34	0.61±0.04	0.80±0.05	1.50±0.09	1.33±0.08
θ_{qf}	−51	0.18±0.03	0.15±0.02	0.39±0.05	0.38±0.05
$\theta_{qf}+17$	0	1.77±0.13	1.35±0.07	3.89±0.14	4.88±0.14
$d\sigma/d\Omega_{\pi^0}$ (mb/sr)		1.65±0.19	2.36±0.18	4.43±0.20	5.04±0.14

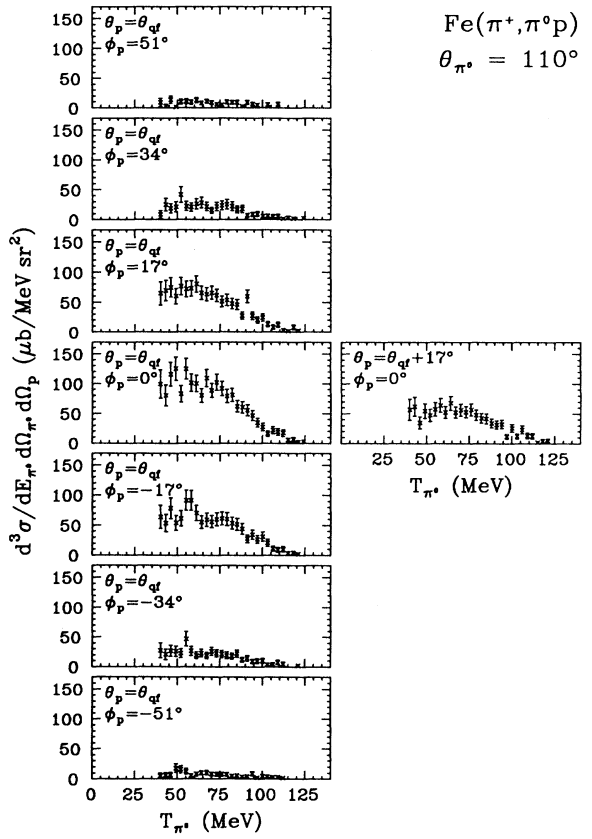

FIG. 14. Energy spectra obtained at $\theta_{\pi^0}=110°$ using the Fe target. The position of each proton telescope is indicated by the angles θ_p (measured in the scattering plane) and ϕ_p (measured perpendicular to the scattering plane). The normalization uncertainty (10%) is not included in the figure.

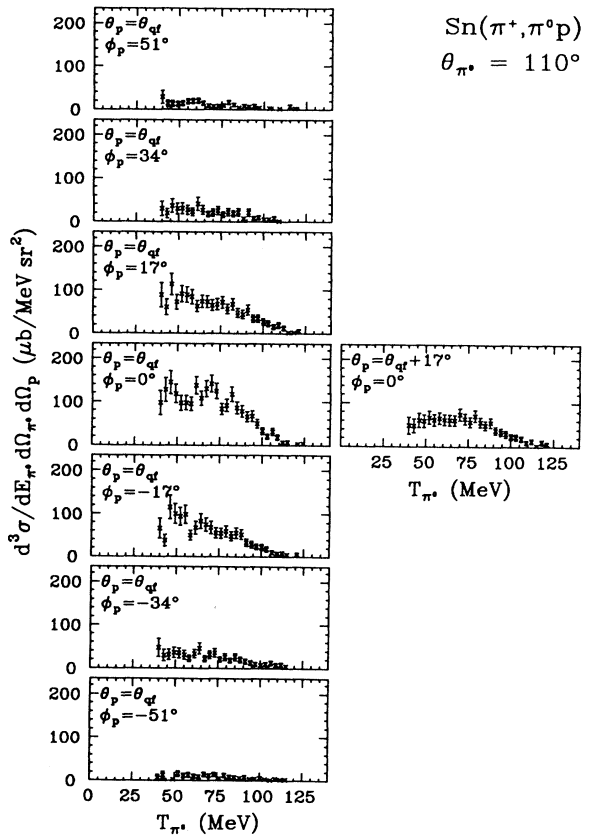

FIG. 15. Energy spectra obtained at $\theta_{\pi^0}=110°$ using the Sn target. The position of each proton telescope is indicated by the angles θ_p (measured in the scattering plane) and ϕ_p (measured perpendicular to the scattering plane). The normalization uncertainty (10%) is not included in the figure.

TABLE IV. Integrated cross sections $d^2\sigma/d\Omega_{\pi^0}d\Omega_p$ and $d\sigma/d\Omega_{\pi^0}$ for all targets. All measurements were made at $\theta_{\pi^0}=110°$. The position of each proton telescope is indicated by the angles θ_p (measured in the scattering plane) and ϕ_p (measured perpendicular to the scattering plane). Only the measurements made at $\theta_p=\theta_{qf}$ were used in calculating $d\sigma/d\Omega_{\pi^0}$. There is a normalization uncertainty of 9% for the ^{16}O data and 10% for data from the other targets in addition to the uncertainties quoted in the table.

		$d^2\sigma/d\Omega_{\pi^0}d\Omega_p$ for (π^+,π^0p) at $\theta_{\pi^0}=110°$ (mb/sr²)			
θ_p (deg)	ϕ_p (deg)	^{16}O	Fe	Sn	Pb
θ_{qf}	51	0.40±0.08	0.51±0.06	0.79±0.10	0.94±0.14
θ_{qf}	34	1.33±0.09	1.28±0.15	1.45±0.17	1.50±0.24
θ_{qf}	17	5.17±0.22	3.91±0.22	4.56±0.27	4.29±0.36
θ_{qf}	0	6.89±0.22	6.06±0.31	6.89±0.36	7.51±0.59
θ_{qf}	−17	4.82±0.22	3.85±0.20	4.18±0.31	4.33±0.39
θ_{qf}	−34	1.50±0.09	1.42±0.12	1.93±0.23	1.83±0.23
θ_{qf}	−51	0.39±0.05	0.49±0.06	0.60±0.11	0.72±0.15
$\theta_{qf}+17$	0	3.89±0.14	3.14±0.15	3.85±0.23	4.25±0.39
$d\sigma/d\Omega_{\pi^0}$ (mb/sr)		4.43±0.20	3.44±0.24	3.69±0.35	3.30±0.40

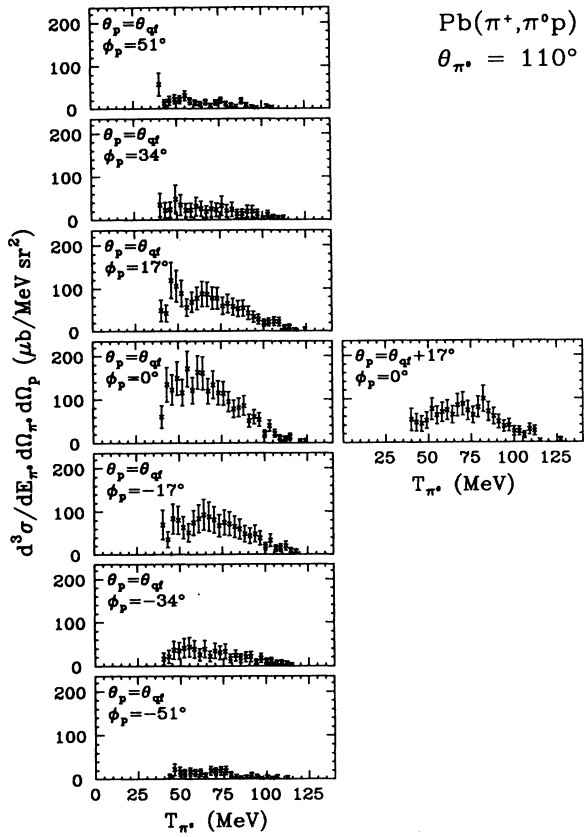

FIG. 16. Energy spectra obtained at $\theta_{\pi^0}=110°$ using the Pb target. The position of each proton telescope is indicated by the angles θ_p (measured in the scattering plane) and ϕ_p (measured perpendicular to the scattering plane). The normalization uncertainty (10%) is not included in the figure.

ly low fraction of p-shell removal events indicates that, even though the cross sections show quasifree characteristics, processes involving initial- and final-state interactions must also be important.

The angular dependence of the $^{16}O(\pi^+,\pi^0 p)$ reaction is illustrated in Fig. 20, which shows the quasifree part of the integrated cross sections $d\sigma/d\Omega_{\pi^0}$ for the $^{16}O(\pi^+,\pi^0 p)$ reaction, both for the case of a p-shell cut on the removed nucleon and the case of no such cut (cf. Tables II and III). Also shown is the free $\pi^+ + n \rightarrow \pi^0 + p$ cross section,[14] which has been scaled to go through the data point at $\theta_{\pi^0}=130°$ for both sets of data. Our results indicate a qualitative agreement between the angular distribution of the $^{16}O(\pi^+,\pi^0 p)$ cross section and that of the corresponding free reaction at backward π^0 angles. However, our most forward measurement, at $\theta_{\pi^0}=70°$, yields a significantly suppressed cross section compared to the free reaction. This feature has been noted previously for $(\pi^{\pm},\pi^0)$ data,[13] and it is believed to be related to final-state interaction effects on the forward-going pion and to Pauli-suppression effects on the low-energy proton.

We may use our data to obtain an estimate of the fraction of the $(\pi^+,\pi^0 p)$ cross section that can be assigned to the quasifree single-charge-exchange process. A careful assessment would require a more complete determination of the angular correlation, particularly of the part we associate with other than quasifree processes. Assuming that the flat background used in the fits extends throughout all directions, we find that the quasifree part of the integrated cross sections $d\sigma/d\Omega_{\pi^0}$ in the case of p-shell nucleon removal (Fig. 17) accounts for 53%, 79%, 74%, and 85% of the total (quasifree plus nonquasifree) cross section at π^0 angles 70°, 80°, 110°, and 130°, respectively. The uncertainties in these values are substantial, but our data still indicate a dominance of a quasifree re-

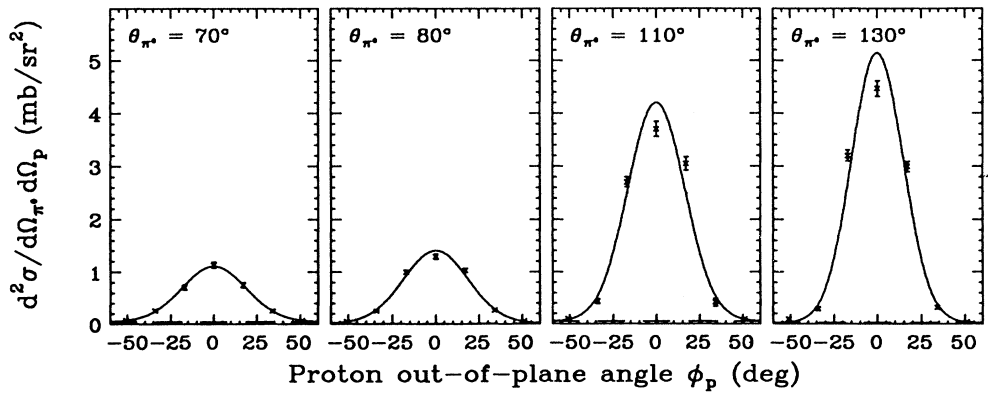

FIG. 17. p-shell nucleon removal cross sections for $^{16}O(\pi^+,\pi^0 p)$ for all setups. The data are from Table II (all telescopes at $\theta_p=\theta_{qf}$). The normalization uncertainty (15%) is not included in the figure. The solid lines are Gaussian fits to the data [added to a constant background (dashes)].

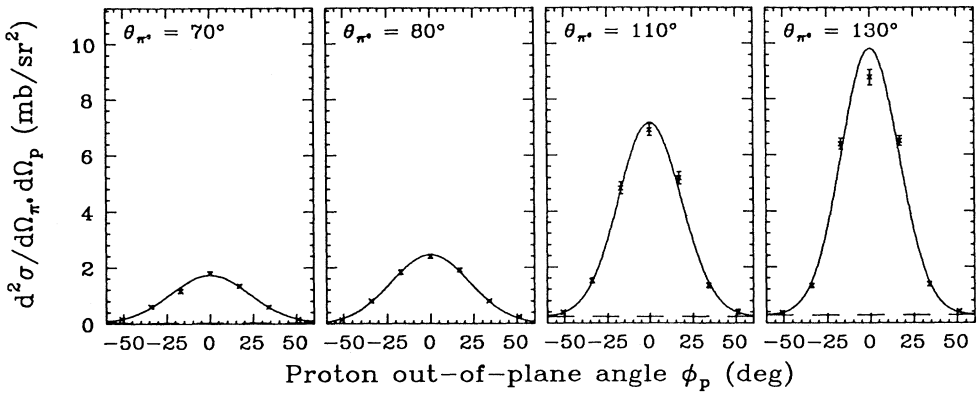

FIG. 18. Complete cross sections for $^{16}O(\pi^+,\pi^0 p)$ for all setups. The data are from Table III (all telescopes at $\theta_p=\theta_{qf}$). The normalization uncertainty (9% for $\theta_{\pi^0}=70°$ and 110° and 8% for the other measurements) is not included in the figure. The solid lines are Gaussians fits to the data [added to a constant background (dashes)].

action mechanism in the $^{16}O(\pi^+,\pi^0 p)$ reaction for p-shell nucleon removal. Moreover, the quasifree contribution appears to increase with π^0 angle, as one would expect considering the effects of final-state interactions. For the various targets used at $\theta_{\pi^0}=110°$ (Fig. 19), we find the quasi-free part of the integrated cross sections to be 59%, 41%, 32%, and 25% for ^{16}O, Fe, Sn, and Pb, respectively. Clearly, the more complex the nucleus, the more the $(\pi^+,\pi^0 p)$ cross section is influenced by initial- and final-state interactions.

V. COMPARISON TO OTHER COINCIDENCE MEASUREMENTS

The $^{16}O(\pi^\pm,\pi^\pm p)$ reaction has been studied at the Paul Scherrer Institute (PSI formerly SIN) at 163 MeV.[18] These measurements constitute the only set of $(\pi^\pm,\pi^\pm p)$ data suitable for direct comparison to our work. However, because each proton detector used in the PSI experiment spanned a much larger solid angle than those used for our $(\pi^+,\pi^0 p)$ measurements, it was necessary to reanalyze the PSI data (imposing geometric acceptances similar to those of our proton telsecopes) before comparisons could be made.[19] From this reanalysis we obtained coincidence cross sections for events in which p-shell nucleons were ejected into angular regions corresponding to our central proton telescope and its three nearest neighbors (all 17° away). Two pion scattering angles were common to the two experiments, and results for these angles with the different geometric cuts are shown in Figs. 21–24. Note that in each figure the vertical axes are scaled 9:1:2, corresponding to the cross-section ratios expected from (Δ-resonance-dominated) isospin coupling alone.

Comparing our 130° spectra to those for charged-pion measurements, we note that the $(\pi^+,\pi^+ p)$ and $(\pi^+,\pi^0 p)$

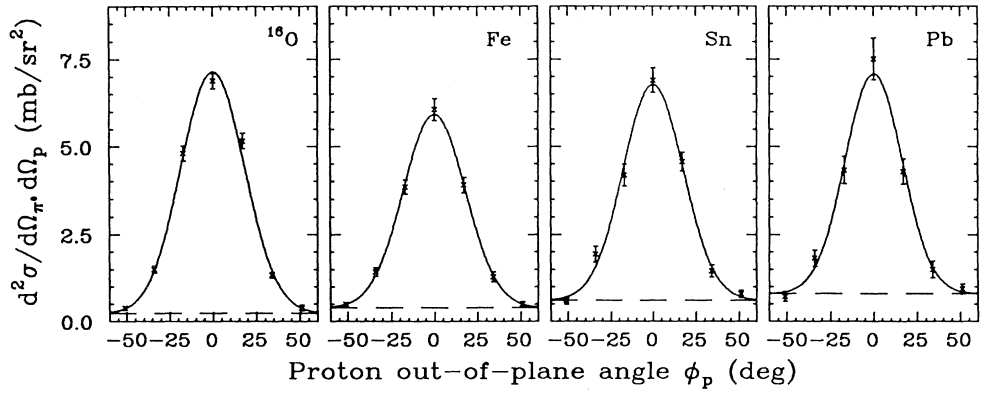

FIG. 19. Cross sections for the $(\pi^+,\pi^0 p)$ reaction on various targets at $\theta_{\pi^0}=110°$. The data are from Table IV (all telescopes at $\theta_p=\theta_{qf}$). The normalization uncertainty (9% for the oxygen data and 10% for data from the other targets) is not included in the figure. The solid curves are Gaussian fits to the data [added to a constant background (dashes)].

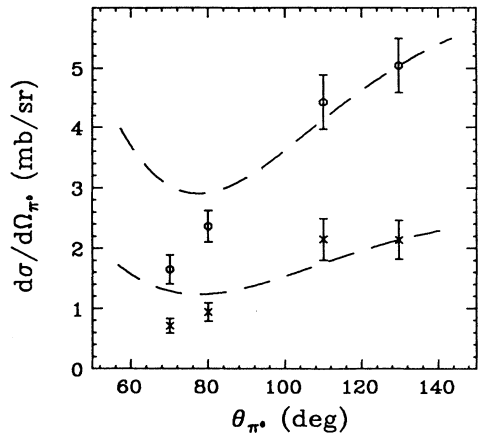

FIG. 20. Integrated cross sections $d\sigma/d\Omega_{\pi^0}$ for the $^{16}O(\pi^+,\pi^0 p)$ reaction. The figure shows our results when all ejected protons are accepted (circles) and when only p-shell protons are included (crosses). The normalization uncertainty is included in the figure. The dashed curves both represent the free πN single-charge-exchange cross section (Ref. 14). They have been scaled (by 1.26 and 0.54, respectively) to go through the data points at $\theta_{\pi^0}=130°$.

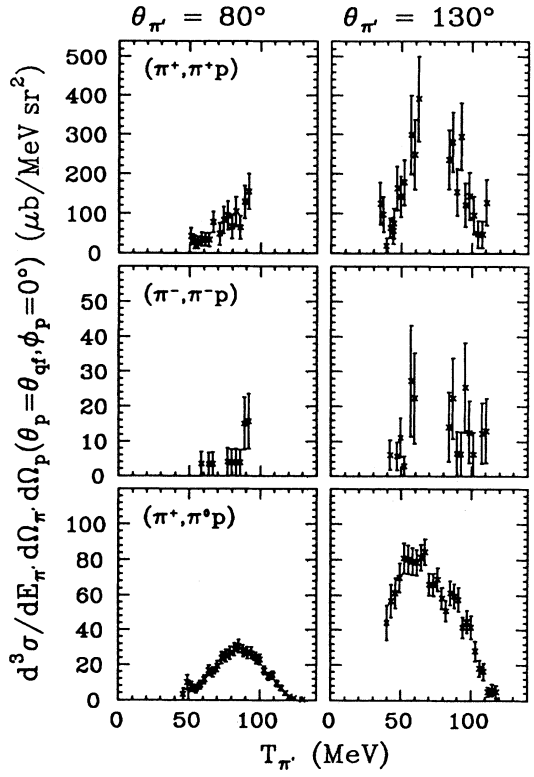

FIG. 21. Comparison of our $^{16}O(\pi^+,\pi^0 p)$ measurements (third row) to PSI 163-MeV $^{16}O(\pi^\pm,\pi^\pm p)$ results (Refs. 18 and 19) (upper two rows). All data are for events detected by the proton telescope at the conjugate quasifree angle ($\theta_p=\theta_{qf}$, $\phi_p=0°$). The column to the left is for $\theta_{\pi'}=80°$, and the column to the right is for $\theta_{\pi'}=130°$ (134° for the PSI measurements). The vertical axes are scaled by the corresponding $T=\frac{3}{2}$ isospin coupling ratios 9:1:2 (top to bottom).

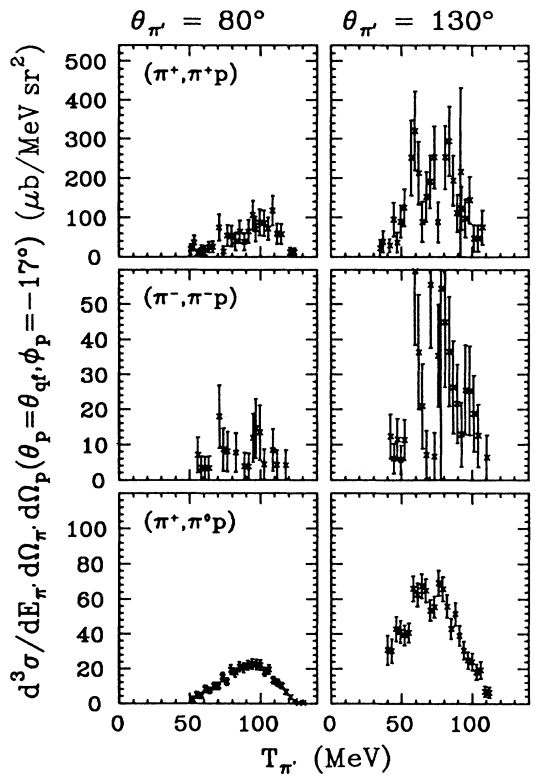

FIG. 22. Comparison of our $^{16}O(\pi^+,\pi^0 p)$ measurements (third row) to PSI 163-MeV $^{16}O(\pi^\pm,\pi^\pm p)$ results (Refs. 18 and 19) (upper two rows). All data are for events detected by the proton telescope at ($\theta_p=\theta_{qf}$, $\phi_\pi=-17°$). The column to the left is for $\theta_{\pi'}=80°$, and the column to the right is for $\theta_{\pi'}=130°$, (134° for the PSI measurements). The vertical axes are scaled by the corresponding $T=\frac{3}{2}$ isospin coupling ratios 9:1:2 (top to bottom).

spectra look roughly the same for all telescopes (that is, the cross-section ratios are roughly equal to the ratios calculated from isospin coupling). This is in accordance with similar observations made at 245 MeV in Ref. 5. It was found there that the ratio of the (π^+,π^+p) to the (π^+,π^0p) cross section were about the same as the isospin calculated ratio at $\theta_{\pi'}=130°$, and that it was clearly smaller than this ratio at $\theta_{\pi'}=60°$. In our case the (π^+,π^+p) and (π^+,π^0p) spectra also appear similar at the more forward angle; there is no apparent relative enhancement of the (π^+,π^0p) process at 80°. These observations are not necessarily in conflict, however. Figure 20 indicates that the behavior at 70° is significantly different from that at 80°, and the observation in Ref. 5 was made at the even more forward angle of 60°. Quantitatively, we have compared our integrated cross sections presented in Table II to integrated cross sections obtained in the same way for the (π^+,π^+p) measurements. Considering the large uncertainties involved, we can only conclude that at both $\theta_{\pi'}=80°$ and 130° the ratios of integrated cross sections $d^2\sigma/d\Omega_{\pi'}d\Omega_p$ of (π^+,π^+p) to (π^+,π^0p) are not in obvious disagreement with the free πN cross-section ratio (which is about 3.9 for both an-

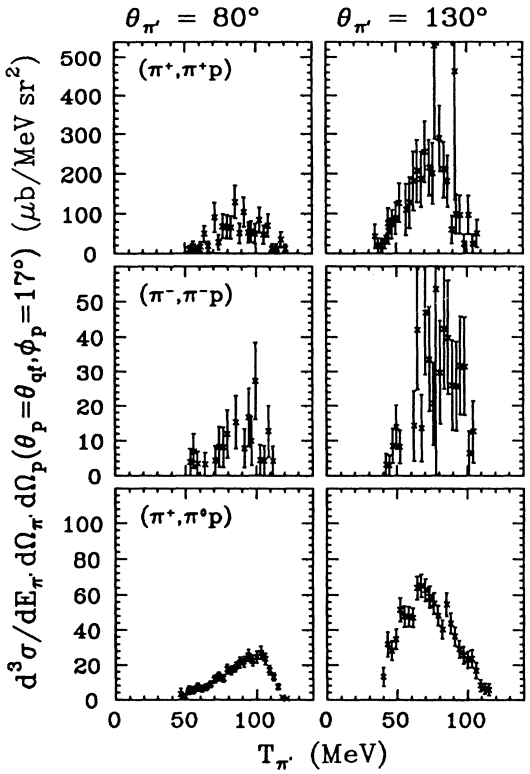

FIG. 23. Comparison of our $^{16}O(\pi^+,\pi^0p)$ measurements (third row) to PSI 163-MeV $^{16}O(\pi^\pm,\pi^\pm,p)$ results (Refs. 18 and 19) (upper two rows). All data are for events detected by the proton telescope at ($\theta_p=\theta_{qf}$, $\phi_p=17°$). The column to the left is for $\theta_{\pi'}=80°$, and the column to the right is for $\theta_{\pi'}=130°$ (134° for the PSI measurements). The vertical axes are scaled by the corresponding $T=\frac{3}{2}$ isospin coupling ratios 9:1:2 (top to bottom).

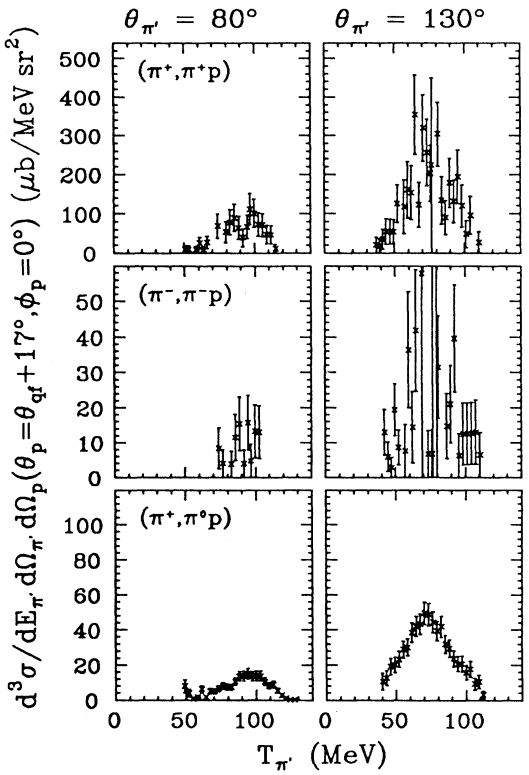

FIG. 24. Comparison of our $^{16}O(\pi^+,\pi^0p)$ measurements (third row) to PSI 163-MeV $^{16}O(\pi^\pm,\pi^\pm p)$ results (Refs. 18 and 19) (upper two rows). All data are for events detected by the proton telescope at ($\theta_p=\theta_{qf}+17°$, $\phi_p=0°$). The column to the left is for $\theta_{\pi'}=80°$, and the column to the right is for $\theta_{\pi'}=130°$ (134° for the PSI measurements). The vertical axes are scaled by the corresponding $T=\frac{3}{2}$ isospin coupling ratios 9:1:2 (top to bottom).

gles[14]). Because of the low statistics, we cannot study the (π^-,π^-p) reaction quantitatively. Qualitatively, cross-section ratios involving (π^-,π^-p) do not appear to be in obvious disagreement with the simple isospin ratios (or with the free πN ratios).

In our A-dependence study, we found that within the sensitivity of our experiment, the cross section for the (π^+,π^0p) reaction varies with A hardly at all. This feature of roughly constant cross section with increasing A is in agreement with earlier observations for the (π^+,π^+p) reaction at the same beam energy.[20] This result is somewhat surprising. The (π^+,π^0) reaction is clearly A dependent,[9,13] and it is not obvious that just including effects of proton distortion can explain all the cancellation of this A dependence.[9]

VI. COMPARISON TO PREDICTIONS OF THE Δ-HOLE MODEL

Theoretical $(\pi,\pi'p)$ cross-section calculations have recently been performed within the framework of the Δ-hole model.[8] Such calculations have also been performed for conditions corresponding to our experiment.[21] The application of the Δ-hole model is thoroughly discussed in Ref. 8. All possible second-order processes are shown in Fig. 25. Diagrams (1)–(3), (5), and (6) correspond to self-energies of pion or delta and are hence already included in distorted-wave impulse approximation (DWIA) calculations. Diagrams (7) (the "direct term") and (8) (the "exchange term") are considered in the Δ-hole model calculations of Ref. 8. Diagram (4) (the "rearrangement process") has the same isospin structure as diagram (7) and is not included in this work.

The upper row of Fig. 26 shows our $^{16}O(\pi^+,\pi^0p)$ results for p-shell nucleon removal obtained using the proton telescope at the conjugate quasifree angle (from Fig. 4) along with the corresponding Δ-hole model predictions. The calculations assumed a pointlike proton detector, while our proton telescopes each span about 8.5 msr. This, at least partly, explains why the p-shell structure (that is, the dip near the quasifree energy) is more evident in the calculations than in the data. Moreover, our data are known to have a significant contribution (about 20%) from other processes (mainly s-shell nucleon removal)

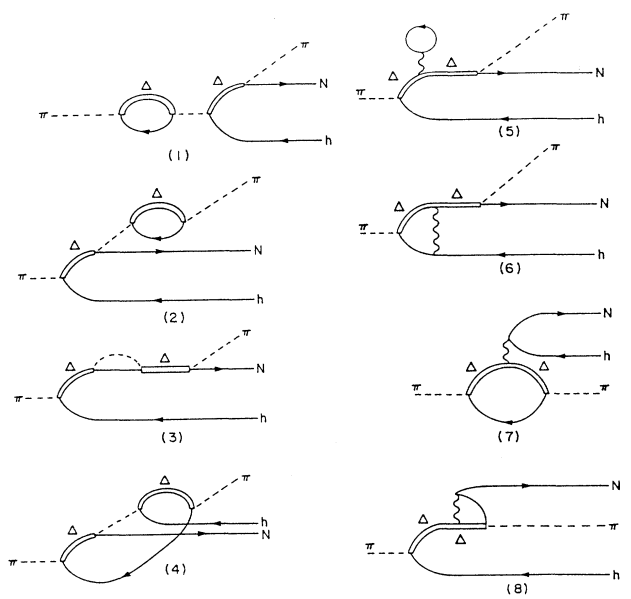

FIG. 25. Diagrams for second-order processes in the framework of the Δ-hole model. These processes are induced by one-pion exchange [(1)—(4)] or the effective Δ-N interaction [(5)—(8)]. The figure is from Ref. 8.

within our p-shell cut. This will also tend to fill in the expected dip. However, we lose a similar amount of true p-shell events, and so the integrated cross sections should not be influenced much by the uncertainties of the p-shell cut. Integrating the theoretical estimates and comparing to our values of $d^2\sigma/d\Omega_{\pi^0}d\Omega_p$ from Table II, we find that the Δ-hole model calculations account for 55%, 64%, 50%, and 54% of the integrated cross sections at π^0 angles 70°, 80°, 110°, and 130°, respectively. The calculations thus underestimate the experimental cross sections by about 30—55 % (our normalization uncertainty of 15% taken into account). The relative constancy of the fraction accounted for at the four π^0 angles indicates that the calculated theoretical angular dependence is consistent with our data. We note that inclusion of the Δ-N interaction term change the cross-section estimates in the correct direction, but by much too small an amount to reach agreement with the data. A similar situation has been observed at 245 MeV.[5,8]

Δ-hole model calculations have also been performed for events detected by the proton telescope outside of the vertical array (which was in the scattering plane 17° farther away from the beam than the central telescope).[21] These calculations are shown in the lower row of Fig. 26. Interestingly, with our 15% normalization uncertainty taken into account, the theoretical estimates now appear

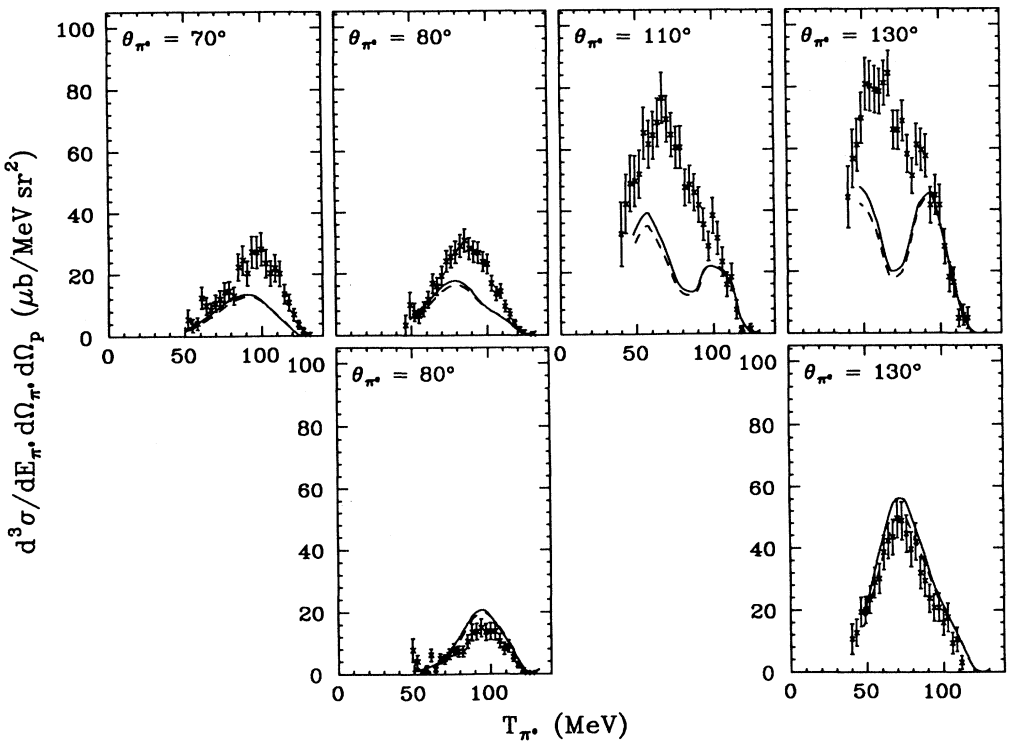

FIG. 26. Our $^{16}O(\pi^+,\pi^0 p)$ results for p-shell nucleon removal compared to predictions of the Δ-hole model. The dashed curves show results of "modified DWIA" calculations, while the solid curves represent full Δ-hole model calculations including the Δ-N interaction (Refs. 8 and 21). The upper row contains the results for the proton telescope at the conjugate quasifree angle, while the lower row is for the proton telescope outside of the vertical array ($\theta_p=\theta_{qf}+17°$, $\phi_p=0°$). There is a 15% normalization uncertainty of the experimental data in addition to the uncertainties shown in the figure.

to be essentially in agreement with our data. Unfortunately, no calculations have been performed corresponding to any of the other proton telescopes. Based on the comparisons in Fig. 26 alone, a possible conclusion is that the Δ-hole model calculations do not reproduce the angular correlation of the ejected particles correctly; our observations suggest that the calculated angular distribution may be too broad. It is also possible that the disagreement exists mainly for the central telescope. Here, at the conjugate quasifree angle, the experimental *p*-shell cross sections are must vulnerable to contributions from other processes (in particular *s*-shell nucleon removal) and final-state interactions. However, as stated above, we do not believe that all of the disagreement can be assigned to this source.

There are two limitations in the theoretical calculations that may need to be investigated further in order to improve the theoretical estimates. First, one possible diagram, the "rearrangement process" [diagram (4) in Fig. 25] is not included. The contribution from this term for $(\pi^+,\pi^0 p)$ is estimated to be 5 times that for $(\pi^-,\pi^- p)$, and 15 times that for $(\pi^+,\pi^+ p)$, and including it may modify the calculated $^{16}O(\pi^+,\pi^0 p)$ cross sections by about 10−20 % at the quasifree peak.[8] Inclusion of the rearrangement process may therefore be important to the understanding of our data, even if it is not crucial to the understanding of the charged-pion channels.

The second limitation in the calculations is the restriction to only the $T_{\Delta N}=1$ channel for the Δ-*N* interaction. This channel corresponds to two-nucleon absorption of pions. Recent experiments have shown that multinucleon absorption is also important,[22] and this may be related to the $T_{\Delta N}=2$ channel.[8] The $T_{\Delta N}=2$ channel may therefore contribute an essential part to the understanding of our cross-section spectra.

VII. SUMMARY AND CONCLUSIONS

We have found that the $(\pi^+,\pi^0 p)$ reaction always has a large contribution from quasifree reactions. As expected, the relative contribution decreases with A (from about 60% for $A=16$ to about 25% for $A=208$ at $\theta_{\pi^0}=110°$). For ^{16}O, this relative contribution is clearly larger when only *p*-shell nucleon removal events are considered than when all $\pi^0 p$ events are included. 40−50 % of the quasifree $\pi^0 p$ coincidence events are due to *p*-shell proton removal. This value suggests that the non-*p*-shell removal part of the cross sections may have a substantial contribution of quasifree events which also involve initial- and final-state interactions.

The $^{16}O(\pi^+,\pi^0 p)$ cross section at forward π^0 angles is considerably lower (more than a factor 2) than those at backward angles, even more so than expected from the angular dependence of the free $\pi^+ n$ single-charge-exchange cross section. The discrepancy with respect to the free cross section is most likely due to final-state interactions experienced by the forward ejected π^0's.

The cross section for the $(\pi^+,\pi^0 p)$ process is almost constant over the range of nuclei studied (from $A=16$ to 208).

Within the statistics of the present experiments, the cross-section ratios of the $(\pi^+,\pi^+ p)$, $(\pi^-,\pi^- p)$, and $(\pi^+,\pi^0 p)$ reactions at $\theta_{\pi'}=80°$ and 130° are not in disagreement with ratios calculated from $T=\frac{3}{2}$ isospin coupling (Δ dominance) alone (9:1:2) or with the ratios of the corresponding free πN cross sections. This is in accordance with earlier observations of cross-section ratios in which dramatic deviations from the free ratios were observed only at more forward pion angles than those reached in our experiment.

Present Δ-hole model calculations of the $^{16}O(\pi^+,\pi^0 p)$ reaction (for *p*-shell nucleon removal) underestimate the cross sections at the conjugate quasifree angle by about 30−55 %. It is possible that inclusion of the $T_{\Delta N}=2$ isospin channel and the "rearrangement process" could bring the theoretical estimates in better agreement with the experimental data. Calculations done for one proton telescope 17° away from the quasifree angle are in agreement with our data. On the one hand, this may be due to an especially large contamination of non-*p*-shell removal events in our data at the quasifree angle (this is where the *p*-shell cross sections are most vulnerable to contributions from other processes and final-state interactions); on the other hand, it may suggest that the Δ-hole model calculations do not estimate the width of the angular correlation correctly.

At this point, both theory and experiment for the important $(\pi^+,\pi^0 p)$ reaction could stand improvement. Measurements with more complete angular coverage and better energy resolution would be desirable. Furthermore, we are clearly in need of more theoretical calculations; neither the shape and magnitude of the $^{16}O(\pi^+,\pi^0 p)$ cross-section spectra nor the A dependence of the reaction are yet very well understood.

ACKNOWLEDGMENTS

We thank the LAMPF staff for their assistance in mounting and running the experiment and the Isotope and Nuclear Chemistry Division of the Los Alamos National Laboratory for use of their equipment for our beam flux measurements. We also thank G. Gatoff for his contributions in the early stages of the experiment. We are grateful to G. S. Kyle for providing us with $(\pi^\pm,\pi^\pm p)$ results prior to their publication and to T. Takaki for helpful conversations and for performing Δ-hole model calculations matching the conditions of our experiment. We received valuable assistance in the reanalysis of the $(\pi^\pm,\pi^\pm p)$ data from G. S. Kyle and C. H. Q. Ingram. This work was supported by the U. S. Department of Energy under Contract Nos. DE-AC02-76ER03069 and W-7405-ENG-36, by the U.S. Israeli Binational Science Foundation, and by a grant from the Bat-Sheva de Rothschild Foundation for the Advancement of Science and Technology.

*Present address: Nuclear Physics Laboratory, University of Colorado, Boulder, CO 80309.
†Present address: Paul Scherrer Institute, CH-5234 Villigen, Switzerland.
‡Present address: School of Physics and Astronomy, Tel Aviv University, Ramat Aviv 69978, Israel.
§Present address: VG Systems, Woodland Hills, CA 91367.
**Present address: Los Alamos National Laboratory, Los Alamos, NM 87545.
††Present address: CEBAF, Newport News, VA 23606.
‡‡Present address: SLAC, Stanford University, Stanford, CA 94305.

[1]M. S. Kozodaev, M. M. Kulyukin, R. M. Sulyaev, A. I. Filippov, and Yu. A. Shcherbakov, Zh. Eksp. Teor. Fiz. **38**, 409 (1960) [Sov. Phys. JETP **11**, 300 (1960)].
[2]P. L. Reeder and S. S. Markowitz, Phys. Rev. **133**, B639 (1964).
[3]G. S. Kyle, P.-A. Amaudruz, Th. S. Bauer, J. J. Domingo, C. H. Q. Ingram, J. Jansen, D. Renker, J. Zichy, R. Stamminger, and F. Vogler, Phys. Rev. Lett. **52**, 974 (1984).
[4]J. A. Faucett, B. E. Wood, D. K. McDaniels, P. A. M. Gram, M. E. Hamm, M. A. Oothoudt, C. A. Goulding, L. W. Swenson, K. S. Krane, A. W. Stetz, H. S. Plendl, J. Norton, H. Funsten, and D. Joyce, Phys. Rev. C **30**, 1622 (1984).
[5]S. Gilad *et al.*, Phys. Rev. Lett. **57**, 2637 (1986).
[6]S. Høibråten *et al., Intersections Between Particle and Nuclear Physics,* Proceedings of a Conference held in Rockport, ME, May 14-19, 1988, AIP Conf. Proc. No. 176, edited by G. M. Bunce (AIP, New York, 1988), p. 614.
[7]E. Piasetzky *et al.*, Phys. Rev. Lett. **46**, 1271 (1981); Phys. Rev. C **25**, 2687 (1982).
[8]T. Takaki and M. Thies, Phys. Rev. C **38**, 2230 (1988).
[9]S. Høibråten, Ph.D. thesis, Massachusetts Institute of Technology, 1989; Los Alamos National Laboratory Report No. LA-11582-T, 1989.
[10]H. W. Baer *et al.*, Nucl. Instrum. Methods **180**, 445 (1981).
[11]B. J. Dropesky, G. W. Butler, C. J. Orth, R. A. Williams, M. A. Yates-Williams, G. Friedlander, and S. B. Kaufman, Phys. Rev. C **20**, 1844 (1979).
[12]S. Gilad, Ph.D. thesis, Tel-Aviv University, 1979.
[13]D. Ashery *et al.*, Phys. Rev. C **30**, 946 (1984).
[14]R. A. Arndt and L. D. Roper, Center for Analysis of Particle Scattering, Virginia Polytechnic Institute and State University, Blacksburg, Virginia, Report No. CAPS-80-3, 1983; R. A. Arndt, J. M. Ford, and L. D. Roper, Phys. Rev. D **32**, 1085 (1985); we used solution FA86.
[15]D. F. Measday and C. Richard-Serre, Nucl. Instrum. Methods **76**, 45 (1969).
[16]A. M. Sourkes, M. S. de Jong, C. A. Goulding, W. T. H. van Oers, E. A. Ginkel, R. F. Carlson, A. J. Cox, and D. J. Margaziotis, Nucl. Instrum. Methods **143**, 589 (1977).
[17]J. H. Hubbell, H. A. Gimm, and I. Øverbø, J. Phys. Chem. Ref. Data **9**, 1023 (1980).
[18]G. S. Kyle (private communication). The 163-MeV measurements were made as described for similar 240-MeV measurements in Ref. 3.
[19]The reanalysis was done by G. S. Kyle, S. Høibråten, and C. H. Q. Ingram (unpublished).
[20]E. Piasetzky *et al.*, Phys. Lett. **114B**, 414 (1982).
[21]T. Takaki (private communication).
[22]D. Ashery and J. P. Schiffer, Annu. Rev. Nucl. Part. Sci. **36**, 207 (1986).